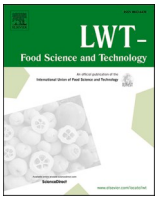
LWT - Food Science and Technology 192 (2024) 115538



Contents lists available at ScienceDirect

LWT

journal homepage: www.elsevier.com/locate/lwt





Structural and textural properties of a novel animal fat-trimming analog based on salted butter and alginate

Chong Teng [a], Da Chen [b], Osvaldo H. Campanella [a,*]

[a] Department of Food Science and Technology, Ohio State University, 2015 Fyffe Road, Columbus, OH, 43210, United States
[b] Department of Animal, Veterinary and Food Sciences, University of Idaho, 875 Perimeter Drive MS 2330, Moscow, ID, 83844, United States

ARTICLE INFO

Keywords:
Animal fat trimming analog
Gelled emulsion
Alginate
Heat stability
Texture
Microstructure

ABSTRACT

The market for meat analogs has been blooming in the recent decade, but fat analogs slowly releasing lipids during cooking have received less attention. A fat-trimming analog based on sodium alginate (Alg) and salted butter (SB) was developed. The influence of salted butter content on the physicochemical properties of the pre-emulsion and the gelled emulsion was studied.

The analog was prepared by homogenizing an Alg dispersion and melted SB, followed by calcium-induced gelation. Rheology showed that pre-gelled emulsions exhibit shear-thinning behavior, and their viscosities, measured at low-shear rates increased, with SB content. After gelation, samples were heat stable and slowly released lipids when heated.

Confocal microscopy showed a typical oil-in-water emulsion structure, with lipid droplets flocculated at higher SB content. Differential scanning calorimetry (DSC) and Fourier-transform infrared spectroscopy (FTIR) tests, respectively revealed no changes in lipid melting/crystallization or in functional groups, indicating unaltered lipids properties due to their physical entrapment in the gelled polysaccharide matrix. Texture profile analysis (TPA) showed decreased cohesiveness, springiness, and chewiness with increased SB content, whereas hardness was first reduced and then increased at 80 g/100 g SB content. The approach used could be a potential solution for producing fat-trimming analogs with improved texture and heat stability.

1. Introduction

Due to the increasing greenhouse gas emission, land and freshwater use of meat production, meat analogs have become an option in consumers' diets, and the thriving market of meat analogs is expected to be valued at over $21 billion by 2025 (Ritchie et al., 2019; Shahbazi et al., 2021). Meat analog is a food product that simulates traditional meat products' aesthetic, sensory, and physicochemical attributes (Bohrer, 2019). It mainly contains plant proteins, lipids, structural agents, and other ingredients (Ishaq et al., 2022). Extensive research has been conducted on protein texturization (Li et al., 2022) but less attention has been given to replacing lipids present in real meat, even though they contribute significantly to meat product juiciness, texture, and flavor.

Most commercial meat analog formulas include plant oils, such as rapeseed oil, sunflower oil, corn oil, etc., as their lipid portion. However, vegetable oil is short of meat-derived volatile compounds that contribute significantly to specific meat flavors (Kołodziejczak et al., 2021). More importantly, liquid vegetable oil is usually responsible for oil leakage (Manzoor et al., 2022). A lipid that could be used and not rejected by individuals that follow a flexitarian diet is butter. Butter contains fatty acids associated with flavor and many health benefits. Approximately 30% of lipids are unsaturated fatty acids, e.g., conjugated linoleic acid (CLA) with health benefits such as inhibitory effects against multistage carcinogenesis, reducing fat mass in overweight humans, increasing anti-inflammatory cytokine and plasma lgA or lgM (Gaullier et al., 2005; Lee et al., 2005; Song et al., 2005). From a functional perspective, the higher melting point of butter is also desired to mimic animal fat-like behavior used in meat products (fat trimmings).

In real fat trimming, the lipid is stored in adipose cells and supported by a network of connective tissue (Dreher et al., 2020). The extracellular scaffold of the network is mainly collagen, a fibrous protein that helps shape and stiffen the tissue to provide mechanical strength (Burla et al., 2020). When heated, the collagen network shrinks and the triple-helical conformation of the collagen protein transitions to that of an amorphous random coil (Flandin et al., 1984). This transition allows a slow release of the liquid lipid during cooking.

* Corresponding author.
E-mail address: campanella.20@osu.edu (O.H. Campanella).

https://doi.org/10.1016/j.lwt.2023.115538
Received 1 January 2023; Received in revised form 10 November 2023; Accepted 12 November 2023
Available online 16 November 2023
0023-6438/© 2023 Published by Elsevier Ltd. This is an open access article under the CC BY-NC-ND license (http://creativecommons.org/licenses/by-nc-nd/4.0/).

To mimic the fat trimming, oleogels have emerged during the last decade as a promising way to solidify oils. During the production of oleogels, the liquid phase (oil) is immobilized by suitable gelation agents (gelators) which convert the former into a solid phase (Park & Maleky, 2020). Although oleogels have shown good potential in controlling phase separation by decreasing oil migration and providing solid-like behavior like conventional animal fat, they often exhibit waxy mouth-feel, lower oxidation stability, negative impact on meltability and digestibility of lipid matrix (Dreher et al., 2021; Martins et al., 2018; Park & Maleky, 2020). Furthermore, oleogels are typically thermal reversible and lack of the ability to control the release of the encapsulated liquid while maintaining elasticity.

An emulsion gel-based delivery system might be one potential option to protect and release lipids (Lu et al., 2019). In this study, sodium alginate was chosen as the gelling agent, as it showed outstanding gelling ability that can be used to encapsulate bioactive compounds such as lycopene, β-carotene, caffeine, etc. (L. Li et al., 2007; Liao et al., 2022; Lin et al., 2022; Nikoo et al., 2018). However, the number of attempts to incorporate hydrophobic compounds, especially at a high portion (>10 g/100 g), has been limited by the hydrophilic nature of the sodium alginate dispersion, which leads to unfavorable stability. In the present study the presence of a little amount of protein in the butter was assumed to be stabilize the pre-gelled emulsions, which is essential to produce a good quality gel. Previous studies showed that a similar concentration of pea protein could emulsify plant oils leading to gelled emulsions with good texture (Teng & Campanella, 2023).

Therefore, the objective of this study was to develop a fat trimming analog by emulsifying salted butter in a sodium alginate dispersion followed by the gelling of the emulsion with a calcium chloride solution and understand the influence of salted butter content on the gelled emulsion. More specifically, the rheology of the pre-gelled emulsion, the changes in the melting/crystallization behavior of the lipids in the gelled state and lipids functional groups, the product microstructure, and its texture profile were investigated.

2. Materials and methods

2.1. Materials

Salted butter (SB) was obtained from a local market, and the protein content was determined to be 0.8 g/100 g with a nitrogen analyzer (Elementar, Long Island, NY, USA, conversion factor was 6.38). Sodium alginate (Alg) was purchased from Landor Trading Co. Ltd. (Montréal, QC, Canada). The alginate has a ratio between mannuronic (M) and guluronic acid (G) ratio, M/G ratio, of 1.5. The M/G ratio is a critical factor affecting the physical properties of alginate suspensions and its resultant gels (Lee & Mooney, 2012). Similar M/G ratios used by other authors and our viscosity results (Fig. 1) indicate that suspensions of these alginates have high viscosity. Calcium chloride (Sigma-Aldrich, St. Louis, MO, USA) and hexane (Fisher Scientific, Waltham, MA, USA) were of analytical grade. Nile red (Technical grade, Sigma-Aldrich) was diluted to 1 mg/mL in acetone (Fisher scientific). Rhodamine B (Rd B, ≥95%, HPLC) grade) was prepared with deionized water at 2 mg/mL.

2.2. Preparation of alginate solution

Sodium alginate was added to deionized water in a capped glass jar to achieve a suspension with a concentration 3 g/dL. The suspension was heated at 70 °C in a water bath for at least 4 h with manual stirring for complete solute distribution. It was then stood at room temperature (20 °C) before use. Typical concentrations of sodium alginate for preparation of emulsions typically range from 1 to 4 g/dL (Li et al., 2020; Lin et al., 2021; Ong et al., 2015), thus a concentration of 3 g/dL was used in the current study. Regarding SB, a range ~30–200 g into a 50 g of alginate suspension was incorporated, which resulted in an oil in water emulsion with a high concentrated dispersed phase.

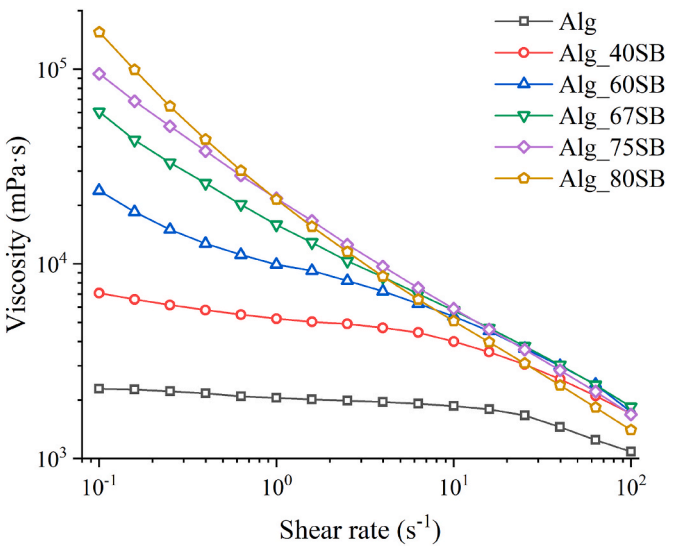


Fig. 1.

2.3. Gel preparation

The internal/dispersed phase was gradually added to the continuous phase to achieve an emulsion with a stable internal phase as described by Manoi and Rizvi (2009). Five grams of melted salted butter (SB, maintained at 70 °C in a water bath) was added to 50 g of the 3 g/dL alginate suspension at 70 °C with manual stirring to form a stable creamy emulsion. Melted SB, at 5 g each time, was then added to the mixture using the same stirring method until the target SB content was reached.

Emulsions with different SB contents (40–80 g/100 g) were prepared and transferred to 50 mL centrifuge tubes (~30 mL per tube). A portion of the emulsion (25 mL) was collected for rheological tests. 20 mL of 1.5 g/dL $CaCl_2$ solution (25 °C) was gradually added to the emulsion in the centrifuge tubes to form a gel. The gels were stored at 4 °C in a refrigerator for 36 h to achieve complete gelation before analysis. Alg_40SB, Alg_60SB, Alg_67SB, Alg_75SB, and Alg_80SB represent systems containing 40 g/100 g, 60 g/100 g, 67 g/100 g, 75 g/100 g, and 80 g/100 SB, respectively. Emulsions and gels were prepared in three batches. The composition of gels was considered identical as the emulsion because phase separation and syneresis were not observed.

2.4. Rheometry

Rheological tests were performed on the emulsions before gelation using a Discovery HR-3 rheometer (TA Instruments, New Castle, DE, USA) with a 40 mm hatched parallel plate to minimize slippage following modified test protocols (Zhao et al., 2022). All tests were performed at 50 °C to maintain the mixture as a liquid. A solvent trap was used to reduce water loss. A flow sweep was conducted with a shear rate ranging from 0.1 to 100 s^{-1} to determine the viscosity of the emulsions before gelling. The flow curves were fitted to the power-law (Eq. 1)

$$\sigma = K\dot{\gamma}^n \tag{1a}$$

where σ is the shear stress (Pa), K the flow consistency index (Pa·s^n), n the power-law index (unitless), and $\dot{\gamma}$ is the shear rate (s^{-1}). n defines the sample rheological behavior; $n = 1$: Newtonian, $n < 1$: shear-thinning and $n > 1$: shear-thickening.

The viscoelastic properties of the gelled samples were tested using a small amplitude oscillatory shear (SAOS) test. First, a strain amplitude sweep ranging from 0.02 to 1000% at a frequency of 1 Hz was performed to identify the sample viscoelastic region. Then, the strain was set at

0.1% (within the linear viscoelastic region), and a frequency sweep was conducted from 0.01 to 100 Hz.

2.5. FTIR

A modified FTIR determination method was used (Aykas et al., 2020). Gelled samples were freeze-dried before FTIR testing to minimize the influence of water. A portable FTIR device (Agilent Technologies, Santa Clara, CA, USA) coupled with a triple-reflection Attenuated Total Reflectance (ATR) sampler was used to record the mid-infrared spectrum. The instrument was equipped with a Zinc Selenide (ZnSe) beam splitter and a thermo-electrically cooled deuterated triglycine sulfate (DTGS) detector. Scans with a wavenumber range 4000–700 cm^{-1} and a resolution of 4 cm^{-1} were used for each sample. 64 scans were adopted to increase the signal-to-noise ratio. The sampling area was cleaned with ethanol and acetone between each measurement to minimize potential mutual contamination, and a background spectrum was recorded after cleaning. Samples (0.5 g) were placed on the sampling surface, and a presser was used to maximize the contact. Agilent MicroLab PC software was used to collect and analyze data.

2.6. Confocal laser scanning microscopy (CLSM)

For CLSM testing samples were stained for lipids and proteins separately following the method described by Teng & Campanella (2023). To stain lipids, melted SB was first spiked with a Nile Red solution (1 mL/dL) before mixing with the alginate solution. The emulsion was then prepared as described in the gel preparation section.

To stain proteins, an aliquot of 0.5 g of the pre-gelled emulsion was collected and mixed with 10 μL of a rhodamine B solution. A drop of the stained liquid mixture was then placed on the glass slide. Then, 0.20 mL of 1.5 g/dL $CaCl_2$ solution was added to the mix. The cover slip was immediately placed over the sample with one edge touching the slide and lowered into place gently. The system was allowed to sit for 10 min for complete gelation; excessive $CaCl_2$ solution was removed using a filter paper. Finally, the coverslip was sealed with epoxy glue and stored at 4 °C in the dark until observation. Microscopic observation was conducted within 24 h after sample preparation with a Zeiss LSM900 Confocal Microscope (Oberkochen, Germany). The excitation wavelengths used were 493 nm and 577 nm for Nile red and rhodamine B-stained samples, respectively.

Particle size (lipid droplet size) analysis was performed with the Fiji software (Laboratory for Optical and Computational Instrumentation, Wisconsin, USA). Confocal microscopy images of Nile red labeled samples were analyzed using the standard ImageJ format. The background was subtracted, and the image was Gaussian blurred and converted into a binary format using the default threshold method included in the software. The "Particle analysis" function was utilized for the analysis, and the region of interest was adjusted manually. To reduce noise, only particles of sizes within 3–20000 μm^2 were considered. Three representative images of each sample were analyzed, and results are presented as particle diameter distributions assuming every particle as a sphere.

2.7. Heat stability

Heat stability of the gelled samples was determined by measuring the weight loss of the gels subjected at temperatures higher than the lipid melting point.

Samples (2 g) were cut from the gel and gently dried with a filter paper to remove extra $CaCl_2$ solution on the surface. After weighting, samples were put in a container in contact with 150 mL of hexane maintained at 50 °C in a water bath for up to 40 min. Hexane was used due to its ability to rapidly dissolve lipids while preserving the gelled alginate. The sample was then removed from the contact with hexane and dried in a fume hood to evaporate hexane excess. The weight after the treatment was recorded. Mass loss was calculated as:

$$Mass\ loss(\%) = \frac{W_0 - W_t}{W_0} \times 100 \quad (1b)$$

where W_0 is the sample weight before treatment and W_t is the sample weight after treatment.

2.8. Differential Scanning Calorimetry (DSC)

DSC tests were conducted on gelled emulsions using a multi-cell DSC (MCDSC) instrument (TA instruments, New Castle, DE, USA). 150 mg of gelled samples were loaded in the instrument ampoules and sealed for testing. An empty ampoule was used as reference. During operation, the MCDSC system was purged with compressed air. Before scanning, the sample was first heated and equilibrated at 70 °C for 300 s to eliminate thermal history. Then, a cooling curve was conducted by first cooling the sample to −20 °C at a rate of 2 °C/min, followed by holding the sample at −20 °C for 300s. Finally, the sample was heated from −20 °C to 100 °C at 2 °C/min. Melting points and their associated enthalpies were determined from the heat flux versus time curves using TRIOS software.

2.9. Texture profile analysis (TPA)

A TPA test was conducted using a TAxT2i texture analyzer (Stable micro system, Godalming, Surrey, UK). A cylindrical sample (1.5 cm height and 1.8 cm diameter) was prepared using a cylindrical cutter. Samples were allowed to stand at room temperature for at least 30 min for temperature equilibration before testing. A flat plate with a diameter larger than the diameter of the samples was used as the testing probe. The piece was vertically placed on the base, and vegetable oil was applied on the compression plate to minimize friction on the plates. A modified double compression test was performed following Mattice and Marangoni (2020). The test speed was 2 mm/s, the trigger force was 10 g, the wait time between two compressions was 5 s, and the maximum strain achieved was 50%. Data was collected using Exponent Connect software (Stable micro system). At least six replicates were performed for each sample. Hardness, cohesiveness, springiness, and chewiness were calculated from the force versus time-curve (Eroglu et al., 2015).

2.10. Statistical analysis

Analysis of variance (one-way and two-way ANOVA) and Tukey's test were conducted to test significant differences using OriginPro (Origin Lab, Northampton, MA, USA). $P < 0.05$ was considered statistically significant.

3. Results and discussions

3.1. Rheometry

Flow curves of pre-gelled emulsions for different SB contents are shown in Fig. 1, and the values of the fitted coefficients using the power

Table 1
Power-law fitting parameters of the emulsions with different SB content.

	n	K	R^2
Alg	0.912 ± 0.011	2.037 ± 0.057	0.9978
Alg_40SB	0.820 ± 0.016	5.182 ± 0.195	0.9951
Alg_60SB	0.664 ± 0.012	10.354 ± 0.306	0.9953
Alg_67SB	0.518 ± 0.007	17.159 ± 0.288	0.9975
Alg_75SB	0.426 ± 0.006	22.673 ± 0.327	0.9972
Alg_80SB	0.339 ± 0.017	24.820 ± 1.046	0.9643

Data shown as estimate mean ± standard error. Alg, Alg_40SB, Alg_60SB, Alg_67SB, Alg_75SB, Alg_80SB represent alginate solution (3 g/hg), emulsions made of alginate solution and 40, 60, 67, 75, 80 g/hg salted butter, respectively.

law model are displayed in Table 1. All samples showed a good fitting ($R^2 > 0.95$). It must be noted that the viscosity measured at low shear rates increases significantly with the SB content, likely due to the higher volume of dispersed fat and the presence of lipid droplets/particles of larger sizes with increased SB content (shown in CLSM results).

At the testing temperature, SB is melted and the presence of larger droplets at high SB concentration and the higher concentration of the dispersed phase result in larger resistance to flow due to the physical interaction between droplets, leading to high viscosity. Additionally, the power-law index *n* decreased with increase in SB content, indicating a more pseudoplastic behavior.

Conversely, when shear rate was higher, the viscosity of the samples converges to similar values at a shear rate of 100 s^{-1}, indicating that droplet-droplet or droplet-continuous medium interactions had less effect on the viscosity at high shear rates, likely due to disrupted lipid droplets subjected to high shear rates. Alignment of the Alg molecules or aggregates may also decreases the viscosity of dispersions at high shear rates. A similar shear-thinning phenomenon was reported for alginate solutions (Rezende et al., 2009).

Fig. 2A shows strain sweep tests indicating that the alginate solution is a highly viscous liquid with loss moduli (G″) significantly higher than the elastic moduli (G′). The difference between these parameters decreased with increase in the SB concentration, and for SB concentrations of 67 g/100 g or higher pre-gelled emulsions became more elastic with G' > G". From the strain amplitude sweep tests could be observed that alginate samples without SB exhibited a wider strain amplitude range in which the samples exhibited a linear viscoelastic behavior. In other words, changes of sample structures with the addition of SB result in samples with a more elastic behavior but that were more significantly affected by strain. With the addition of SB, values of G″ increased to ~30 Pa for all samples, whereas increase of G' showed more significant dependence on the SB content, reflecting the major influence of SB on the elasticity of the samples.

A frequency sweep at a strain of less than 5% (strain at which all the samples exhibited linear behavior) was conducted and results are illustrated in Fig. 2B. G′ and G″ of all samples increased with frequency. G″ of Alg was greater than G′ in all tested frequency ranges, reflecting a dominant viscous behavior. With the addition of SB samples became more elastic. At the low-frequency range G′ was lower than G″ for Alg_40SB, but it exceeded G″ at a higher frequency. When the SB content was further increased (e.g., Alg_60SB), G′ became slightly higher than G″ at low frequencies and significantly higher at high frequencies (>25 Hz). For SB content higher than 60 g/100 g, G′ was always higher to G″, and the differences between G′ and G″ became more significant, especially at a lower frequency.

3.2. FTIR

FTIR was used to reveal changes in relevant functional groups during gel formation. The FTIR spectra of SB (control), Alg, and gelled Alg emulsions at different SB concentrations are shown in Fig. 3. The signal of Alg was much weaker compared to the rest of samples because the gel became brittle after freeze-drying and converted into a powder. The maximum allowed pressure used to prepare the sample was not able to fully compact the powder and the sampling contact area was reduced. Thus, the Alg spectrum was rescaled to overcome the measured low intensity. Although samples were freeze-dried, water O–H stretching motions (3200-3600 cm^{-1}) were still present, indicating the presence of some residual water in the dried samples. Spectra displayed signature carboxylate antisymmetric stretching at 1592 cm^{-1} and a symmetric stretching at 1414 cm^{-1}. Peaks at 1077 and 1009 cm^{-1} are associated with C–O–C groups. COOH and = C–H groups are responsible for peaks around 937 and 815 cm^{-1}, respectively. Other researchers obtained similar results (Kianersi et al., 2021; Lawrie et al., 2007).

By SB addition at different concentrations, a gradual transition to the SB spectrum was observed without significant peak shifts. Non-observable new peaks different than those belonging to SB and Alg were observed, indicating that no chemical modification occurred during gelation, and the chemical properties of SB remained unchanged. Within samples containing SB, the lipid signals became dominant and with increased SB concentration gradually masked the Alg signal. Detailed peak assignment for SB is shown in Table 2. Peaks were in good accordance with the spectrum of milk butter reported (Bodner &

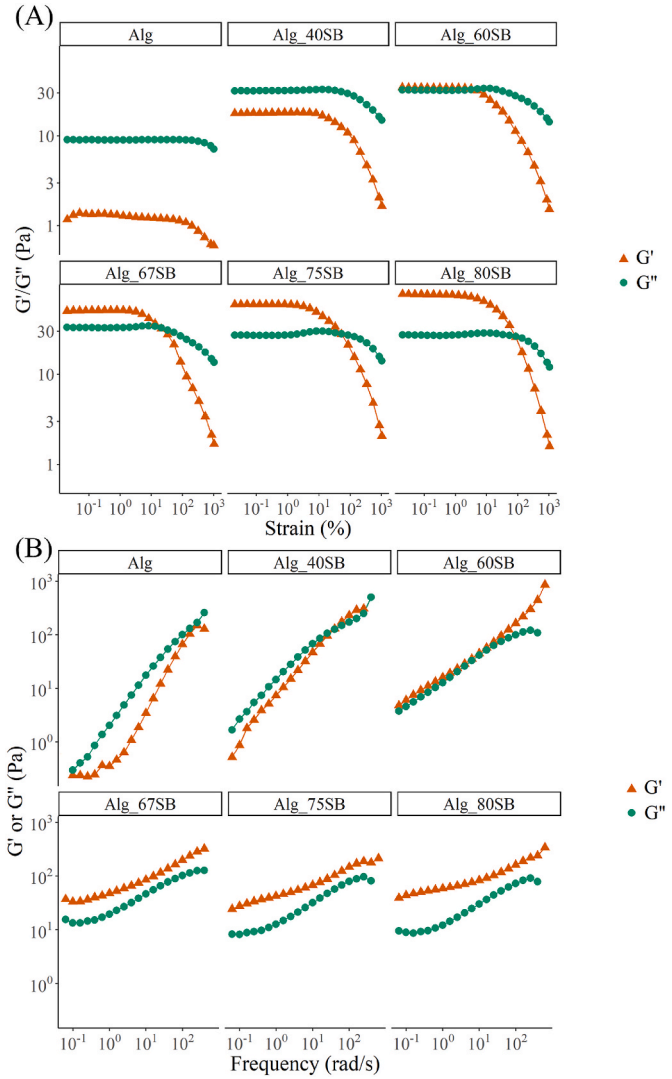


Fig. 2.

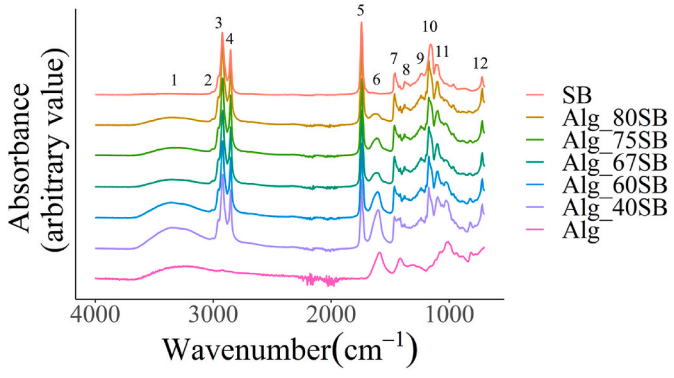


Fig. 3.

Table 2
FTIR peak assignment for salted butter (SB).

Peak number	Wavenumber (cm^{-1})	Vibration
1	3300	O–H symmetric stretching of water
2	3005	C═CH stretching of cis unsaturation
3,4	2922, 2853	Methylene ($–CH_2$) group stretching
5	1742	Carbonyl (C═O) stretching of the ester bond of triglyceride
6	1650	cis C═C or C═O stretching
7	1459	CH_2 and CH_3 bending of aliphatic chains
8	1377	CH_3 symmetric bending
9, 10	1235, 1159	C–O stretching in esters
11	1112	C–O–C stretching in ester linkages
12	721	$–CH_2$ rocking and out of plane vibration of *cis*-disubstituted olefins

Scampicchio, 2020). The presence of peaks around 1650 cm^{-1} is likely to be due to the cis C═C or carbonyl group (C═O) stretching (amide I band from protein). However, the peak around 1591 cm^{-1} was only present in gelled samples containing SB but not pure SB. Therefore, it would correspond to the carboxylate antisymmetric stretching present in alginate, as reported, and not the N-acetylated bending (amide II band) from the protein (Sarmento et al., 2006). Although the butter protein content was about 0.8 g/100 g, its corresponding vibration signals were not identifiable in SB or samples containing SB.

3.3. CLSM

Fig. 4 shows the distribution of lipids and proteins in gels with SB different content. Nile red-stained samples reveal clearly how the lipid morphology changed as a function of the SB content. The sample with the least SB content (Alg_40SB) shows regular spherical lipid droplets within the dark background (gelled sodium alginate). As the lipid content increases, droplets aggregate and deform into more irregular shapes, with the presence of still tiny droplets. With a SB content reached of 80 g/100 g, no clear SB spherical droplets were observed. Instead, lipid flocculation became predominant, and the system appeared to be a W/O emulsion. The absence of obvious spherical droplets in the Alg_80SB sample could be due to the high-volume ratio of the lipid phase close to 0.74, which is the threshold of a potential internal phase inversion.

When the internal/dispersed phase (in this case, SB) is mixed with the hydrophilic polysaccharide solution, the lipid tends to flocculate and separate from the mixture, leading to what is known as the "oil off" phenomenon. This effect was observed when only the lipid portion of SB was mixed with the alginate solution even in the same way as the current study in our preliminary experiments. In addition, when the SB were added directly to the system at one time, phase separation would occur, even using a homogenizer. This might be caused by the generation of droplets of too small sizes, and the protein present in the SB would not be enough to support the system emulsification. Thus, achieving a stable gel relies on the inclusion of an emulsifier and the choice of an appropriate emulsion preparation technique. Other researchers adopted a similar preparation method in which the internal/dispersed phase was gradually added to achieve an emulsion with a stable low internal phase (Manoi & Rizvi, 2009).

Therefore, the stability of the emulsion in this study is primarily attributed to the presence of a small amount of protein (0.8 g/100 g) present in SB which acts as an emulsifier. The preparation method adopted in this work included the gradual addition of oil by applying low shear, which allowed enough time for protein to distribute around the droplet interface to prevent creaming. A similar study focusing on the preparation of fat trimming analogs using vegetable oils showed that a stable emulsion cannot be achieved if a similar amount of protein is not added (Teng & Campanella, 2023).

Proteins were roughly distributed in the space absent of lipid, especially for gels of low SB levels (Fig. 4). For Alg_40SB, it was noted that proteins (right plot) were evenly distributed in the aqueous alginate solution and were almost absent absorbed to the droplet interfaces. This result indicates that the protein naturally present in SB was mainly separated from the lipids during the mixing of the melted SB and the alginate solution. Aqueous phase's homogeneity of protein was also reported for a dilute emulsion system stabilized by oat protein isolate (Zhang et al., 2015). However, as SB content increased, small aggregates of proteins within the lipid droplets became noticeable, although the concentrations of protein were much higher in the aqueous phase. This might be due to the disruption of lipid droplets when a more vigorous shear action was applied during sample preparation, and flocculation with the added melted SB. This structure was different from a system containing a much higher emulsifier (protein) concentration, where high concentration of butterfat (80 g/100 g) showed less aggregation in the presence of 4 g/100 g textured whey protein isolate, and the protein did not appear to penetrate the lipid droplets (Ruttarattanamongkol et al., 2015).

The lipid droplet size distribution is shown in Fig. 5. As the flocculated droplets in Alg_80SB exceeded the area of a single image, the average droplet size was not able to be calculated. The average droplet size increased slightly with increased SB content, resulting from both flocculation and the generation of smaller droplets. In comparison, these gels had a larger average droplet size than fat globules in homogenized milk (Gallier et al., 2010) due to the lower applied shear.

3.4. Heat stability

Data showed that free lipid (only SB) was completely melted and dissolved in hexane at 50 °C. Therefore, if the solvent cannot extract lipids from the gelled sample at high temperatures (above the melting point of the lipid) in a reasonable time, the lipid entrapment could be considered successful. Traditional total lipid content measurements are not appropriate because during the sample preparation for the test the structure would be destroyed (grind or cut to smaller particles) to fully release the lipid. In this regard, the goal of this test was to extract any dissolvable lipid without mechanically destroying the structure. Although the proposed one-time liquid extraction might not reflect the actual value of lipid release during cooking, it might be efficient enough for comparison purposes on practical applications. Fig. 6 shows the mass loss of each sample as a function of heating time. For comparison it has been reported that during a rendering process, meat products, depending on the fat type, can experience shrinkage and weight loss of up to 50% which is attributed mainly to the loss of fat and moisture (Ayub & Ahmad, 2019).

The mass loss increased with SB content increase and heating time, which was within expectation as the surface lipid content was higher in samples containing higher SB content. The relative decrease of Alg content led to weaker protective gels which favored lipid release. However, the mass loss was low compared to those reported in studies in which olive oil was entrapped only with sodium alginate, which showed significant phase separation at neutral storage conditions (Sato et al., 2014) likely due to the lack of natural emulsifiers in olive oil and as shown by Teng and Campanella (2023) the importance of a emulsifier to produce stable gels. The fact that a more extended period of extraction favored the release of lipid also indicates that the polysaccharide matrix reduced solvent infiltration in the solvent and/or lipid migration. Statistical analysis (two-way ANOVA) shows that the SB content had no interactive effects with heating time. The standard deviation was relatively high due to the sample's irregular shape, which affected the accessibility of the lipid to the solvent.

3.5. Differential scanning calorimetry (DSC)

Crystallization (cooling) and heating curves of gelled samples with different SB content are illustrated in Fig. 7. The cooling curves showed

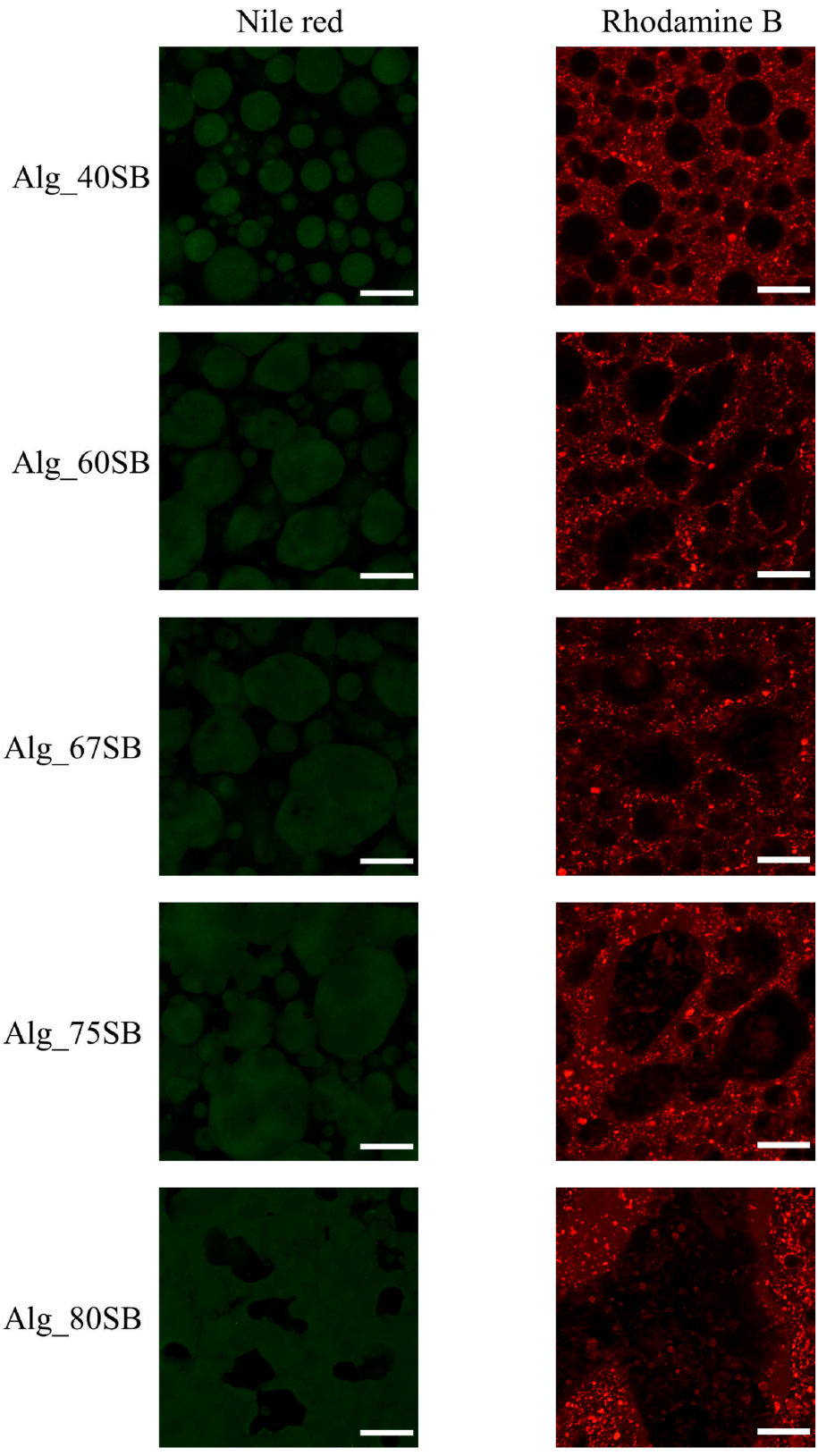


Fig. 4.

two identical exothermic peaks for all samples containing SB at 10.3 °C and 14.6 °C, respectively corresponding to the first order triacylglycerol crystallization (Tomaszewska-Gras, 2012). The enthalpy of gelled SB was lower than that of pure SB and had a rising trend with SB increase. The onset (T_{on}) and crystallization (T_{c1} and T_{c2}) temperatures were slightly higher in the gelled system, likely due to the less interaction between triacylglycerol and protein since most proteins was separated from lipid droplets during sample preparation (Fig. 4). In the sample without of SB (Alg), no peak was observed in the temperature range of lipid crystallization. For all samples except SB, a peak corresponding to

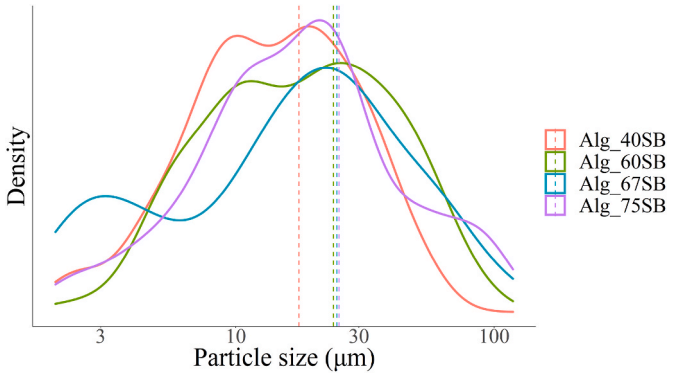


Fig. 5.

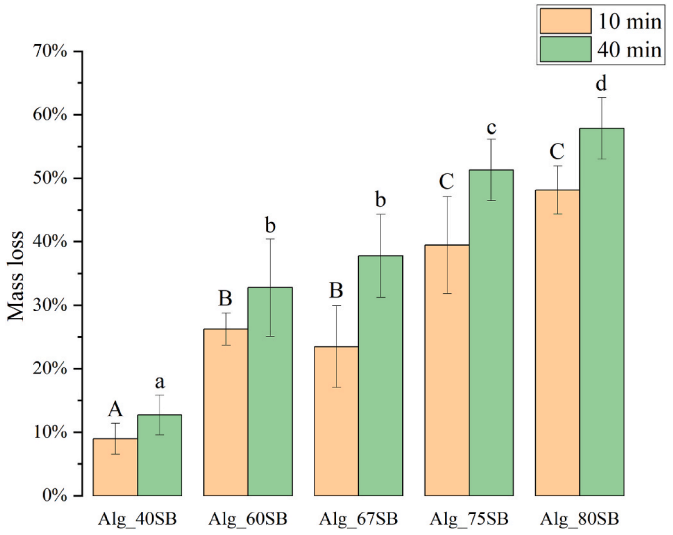


Fig. 6.

the crystallization of water was observed in the temperature range from −17.0 to −14.5 °C. This supercooling phenomenon was also observed in foodstuffs like cheese and high-moisture butter (Gliguem et al., 2009; Tomaszewska-Gras, 2012). The absence of the water crystallization peak in the SB sample suggests that the level of freezable water is low. It can therefore be deduced that although the existence of alginate would affect the crystallization profile of the incorporated SB, this effect is limited. The Alg curve was truncated at high heat flow due to the instrument measurement limit (Fig. 7B).

During heating, a typical melting curve of three melting fractions could be observed in the pure SB sample. The onset temperature of the low melting fraction was at around 7.8 °C, which was higher than that reported in the literature (Smet et al., 2010), probably due to the lower heating rate used during the scanning which might induce more stable crystalline forms (Tomaszewska-Gras, 2012). This peak partly overlapped with the second melting peak (corresponding to median melting point fractions). It is observed that the melting peaks of the median melting fractions were $T_m = 16.7$ °C for both the pure SB and the gelled emulsions. The high melting point fractions had slightly higher T_m in the gelled emulsions than the pure SB sample, indicating the reduced mobility of the lipid when gelled.

These results conclude that alginate would not significantly modify the melting behavior at the tested ratios. In addition, the butter would not fully leak from the system even at temperatures higher than its melting point (the melting peaks ended at around 35 °C), which is in accordance with results from the heat stability test. As for water in the gelled samples, a broad and high peak of ice melting could be observed

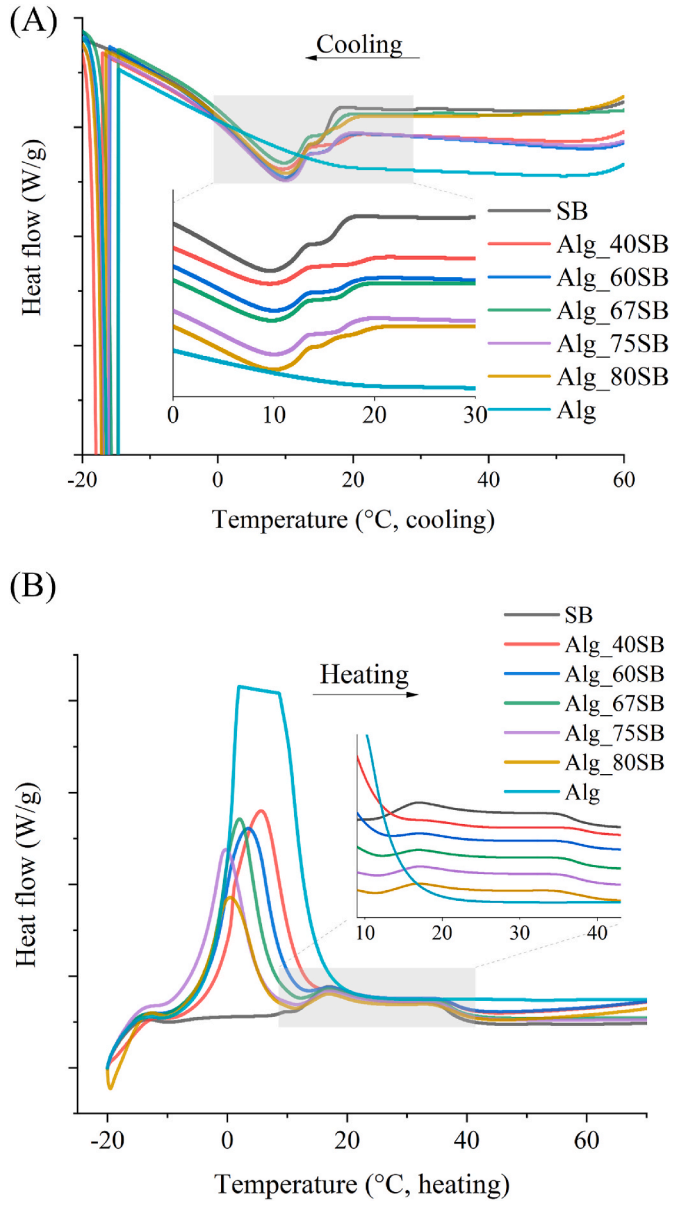


Fig. 7.

in the range −15 to −10 °C in all samples except SB and overlapped with the first melting peak (corresponding to low melting fractions) of the gelled samples. As mentioned, the absence of this ice melting peak in SB was due to its limited freezable moisture content, and water was unable to crystallize before starting the heating scanning. A tendency of reduced ice melting temperature and enthalpy with increased amount of SB has been observed in other studies involving a microemulsion system with an increased internal phase ratio (Chiappisi et al., 2016).

3.6. TPA

TPA is a commonly adopted tool to reflect quantitatively how solid and semisolid samples respond when chewed. The mechanical characteristics are shown in Table 3. For all samples, no identifiable fracture point was recorded. As vegetable oil was used to reduce plate friction during testing, stickiness was not measured. The overall hardness was lower than a cooked steak (6.04 kg) (Caine et al., 2003), which is an ideal comparative sample since the lipid portion alone is often softer than the protein matrix. Hardness decreased with the addition of SB up to 75 g/100 g as the increase of dispersed phase might reduce gel

Table 3
Texture profile analysis (TPA) of gelled trim analog with different salted butter (SB) content.

	Hardness (g)	Cohesiveness	Springiness	Chewiness (g)
Alg	4925 ± 492^{A}	0.56 ± 0.02^{A}	0.58 ± 0.02^{A}	1467 ± 184^{A}
Alg_40SB	4553 ± 213^{A}	0.53 ± 0.01^{AB}	0.49 ± 0.01^{B}	1197 ± 45^{A}
Alg_60SB	3150 ± 214^{BC}	0.48 ± 0.01^{BC}	0.46 ± 0.01^{BC}	826 ± 108^{B}
Alg_67SB	2709 ± 96^{CD}	0.44 ± 0.01^{CD}	0.43 ± 0.02^{C}	635 ± 32^{BC}
Alg_75SB	2251 ± 138^{D}	0.42 ± 0.01^{D}	0.45 ± 0.01^{BC}	426 ± 18^{C}
Alg_80SB	3867 ± 160^{AB}	0.26 ± 0.01^{E}	0.34 ± 0.02^{D}	345 ± 3^{C}

Data are presented as mean ± standard error. Different superscripted letters indicate significant differences ($P < 0.05$). Alg, Alg_40SB, Alg_60SB, Alg_67SB, Alg_75SB, Alg_80SB represent gels made of alginate solution (3 g/hg) and gelled emulsions made of alginate solution and 40, 60, 67, 75, 80 g/hg salted butter, respectively.

strength. This could be due to the unbound relation between the lipid droplet and polysaccharide matrix (Poyato et al., 2014; Sala et al., 2008) as the proportion of gelled alginate is most responsible for hardness, opposite to the emulsion before gelation (Fig. 1). Interestingly, when the SB content reached 80 g/100 g, hardness increased again, which seemed to be inconsistent with the active/inactive filler hypothesis in which the gel stiffness continuously decreases with the increase of the volumetric ratio of inactive particles (Geremias-Andrade et al., 2017; Sala et al., 2009). This phenomenon could possibly be attributed to a possible phase inversion of the emulsion and the crystallization of the lipids. Cohesiveness, springiness, and chewiness showed a constant decrease trend with increases in the SB content. The decline in cohesiveness and springiness indicated that the samples containing higher SB content were more intensively disrupted in the first compression and had less tendency to bounce back.

4. Conclusions

Sodium alginate and salted butter-based gelled emulsions were successfully prepared to mimic the behavior of actual animal fat trimming. The stability of the gelled emulsion stemmed from the presence of protein in salted butter. Incorporating lipids in the alginate matrix did not induce any noticeable functional group change or lipid melting behavior change. The pre-gelled emulsion was viscous when the SB content was low and converted to a viscoelastic material with an increased SB amount. Microscopic images showed that lipids were entrapped in the alginate matrix as droplets, whereas proteins were distributed in the aqueous alginate phase. The lipid droplets would flocculate with increased SB content, while the average particle size would not change significantly. This study provides valuable information on the development of animal fat trimming analogs. However, the preparation method of the gelled emulsion, while efficient, may not adapt to all sorts of lipids and polysaccharide combinations. The product's safety, taste, and nutritional value when subjected to higher cooking temperatures remain undetermined. Future research is therefore recommended to adjust the protein/lipid/polysaccharide type (potentially plant-based) and ratio to better mimic the texture and flavor of natural animal fat considering the various cooking applications and consumer acceptance.

Author statement

Chong Teng: Conceptualization, methodology, investigation, data analysis, writing – original draft, Da Chen: Methodology, investigation, writing – review, and editing, Osvaldo Campanella: Conceptualization, supervision, funding, writing – review, and editing.

Declaration of competing interest

I certified that all authors have seen and approved the final version of the manuscript being submitted. They warrant that the article is the author's original work, hasn't received prior publication, and isn't under consideration for publication elsewhere.

I certified the validity of the research and that the research was not influenced by a secondary interest, such as financial gain or competing interest.

Data availability

Data will be made available on request.

References

Aykas, D. P., Rodrigues Borba, K., & Rodriguez-Saona, L. E. (2020). Non-destructive quality assessment of tomato paste by using portable mid-infrared spectroscopy and multivariate analysis. *Foods, 9*(Issue 9). https://doi.org/10.3390/foods9091300

Ayub, H., & Ahmad, A. (2019). Physiochemical changes in sous-vide and conventionally cooked meat. *International Journal of Gastronomy and Food Science, 17*, Article 100145. https://doi.org/10.1016/j.ijgfs.2019.100145

Bodner, M., & Scampicchio, M. (2020). Analytical authentication of butter using Fourier Transform Infrared spectroscopy coupled with chemometrics. *International Journal of Nutrition and Food Engineering, 14*, 42–49.

Bohrer, B. M. (2019). An investigation of the formulation and nutritional composition of modern meat analogue products. *Food Science and Human Wellness, 8*(4), 320–329. https://doi.org/10.1016/j.fshw.2019.11.006

Burla, F., Dussi, S., Martinez-Torres, C., Tauber, J., van der Gucht, J., & Koenderink, G. H. (2020). Connectivity and plasticity determine collagen network fracture. *Proceedings of the National Academy of Sciences, 117*(15), 8326–8334. https://doi.org/10.1073/pnas.1920062117

Caine, W. R., Aalhus, J. L., Best, D. R., Dugan, M. E. R., & Jeremiah, L. E. (2003). Relationship of texture profile analysis and Warner-Bratzler shear force with sensory characteristics of beef rib steaks. *Meat Science, 64*(4), 333–339. https://doi.org/10.1016/S0309-1740(02)00110-9

Chiappisi, L., Noirez, L., & Gradzielski, M. (2016). A journey through the phase diagram of a pharmaceutically relevant microemulsion system. *Journal of Colloid and Interface Science, 473*, 52–59. https://doi.org/10.1016/j.jcis.2016.03.064

Dreher, J., Blach, C., Terjung, N., Gibis, M., & Weiss, J. (2020). Formation and characterization of plant-based emulsified and crosslinked fat crystal networks to mimic animal fat tissue. *Journal of Food Science, 85*(2), 421–431. https://doi.org/10.1111/1750-3841.14993

Dreher, J., König, M., Herrmann, K., Terjung, N., Gibis, M., & Weiss, J. (2021). Varying the amount of solid fat in animal fat mimetics for plant-based salami analogues influences texture, appearance and sensory characteristics. *LWT, 143*, Article 111140. https://doi.org/10.1016/j.lwt.2021.111140

Eroglu, A., Dogan, M., Toker, O. S., & Yilmaz, M. T. (2015). Classification of Kashar cheeses based on their chemical, color and instrumental textural characteristics using principal component and hierarchical cluster analysis. *International Journal of Food Properties, 18*(4), 909–921. https://doi.org/10.1080/10942912.2013.864673

Flandin, F., Buffevant, C., & Herbage, D. (1984). A differential scanning calorimetry analysis of the age-related changes in the thermal stability of rat skin collagen. *Biochimica et Biophysica Acta (BBA) - Protein Structure and Molecular Enzymology, 791*(2), 205–211. https://doi.org/10.1016/0167-4838(84)90010-4

Gallier, S., Gragson, D., Jiménez-Flores, R., & Everett, D. (2010). Using confocal laser scanning microscopy to probe the milk fat globule membrane and associated proteins. *Journal of Agricultural and Food Chemistry, 58*(7), 4250–4257. https://doi.org/10.1021/jf9032409

Gaullier, J.-M., Halse, J., Høye, K., Kristiansen, K., Fagertun, H., Vik, H., & Gudmundsen, O. (2005). Supplementation with conjugated linoleic acid for 24 months is well tolerated by and reduces body fat mass in healthy, overweight humans. *The Journal of Nutrition, 135*(4), 778–784. https://doi.org/10.1093/jn/135.4.778

Geremias-Andrade, I. M., Souki, N. P. D. B. G., Moraes, I. C. F., & Pinho, S. C. (2017). Rheological and mechanical characterization of curcumin-loaded emulsion-filled gels produced with whey protein isolate and xanthan gum. *LWT, 86*, 166–173. https://doi.org/10.1016/j.lwt.2017.07.063

Gliguem, H., Ghorbel, D., Grabielle-Madelmont, C., Goldschmidt, B., Lesieur, S., Attia, H., Ollivon, M., & Lesieur, P. (2009). Water behaviour in processed cheese spreads. *Journal of Thermal Analysis and Calorimetry, 98*(1), 73–82. https://doi.org/10.1007/s10973-009-0376-x

Ishaq, A., Irfan, S., Sameen, A., & Khalid, N. (2022). Plant-based meat analogs: A review with reference to formulation and gastrointestinal fate. *Current Research in Food Science*.

Kianersi, S., Solouk, A., Saber-Samandari, S., Keshel, S. H., & Pasbakhsh, P. (2021). Alginate nanoparticles as ocular drug delivery carriers. *Journal of Drug Delivery Science and Technology, 66*, Article 102889. https://doi.org/10.1016/j.jddst.2021.102889

Kołodziejczak, K., Onopiuk, A., Szpicer, A., & Poltorak, A. (2021). Meat analogues in the perspective of recent scientific research: A review. *Foods, 11*(1), 105.

Lawrie, G., Keen, I., Drew, B., Chandler-Temple, A., Rintoul, L., Fredericks, P., & Grøndahl, L. (2007). Interactions between alginate and chitosan biopolymers characterized using FTIR and XPS. *Biomacromolecules, 8*(8), 2533–2541. https://doi.org/10.1021/bm070014y

Lee, K. W., Lee, H. joo, Cho, H. Y., & Kim, Y. J. (2005). Role of the conjugated linoleic acid in the prevention of cancer. *Critical Reviews in Food Science and Nutritioneviews in Food Science and Nutrition, 45*(2), 135–144. https://doi.org/10.1080/10408690490911800

Lee, K. Y., & Mooney, D. J. (2012). Alginate: Properties and biomedical applications. *Progress in Polymer Science, 37*(1), 106–126. https://doi.org/10.1016/j.progpolymsci.2011.06.003

Liao, P., Dai, S., Lian, Z., Tong, X., Yang, S., Chen, Y., Qi, W., Peng, X., Wang, H., & Jiang, L. (2022). The layered encapsulation of vitamin B2 and β-carotene in multilayer alginate/chitosan gel microspheres: Improving the bioaccessibility of vitamin B2 and β-carotene. *Foods, 11*(1), 20.

Li, L., Fang, Y., Vreeker, R., Appelqvist, I., & Mendes, E. (2007). Reexamining the egg-box model in calcium−alginate gels with x-ray diffraction. *Biomacromolecules, 8*(2), 464–468. https://doi.org/10.1021/bm060550a

Li, A., Gong, T., Hou, Y., Yang, X., & Guo, Y. (2020). Alginate-stabilized thixotropic emulsion gels and their applications in fabrication of low-fat mayonnaise alternatives. *International Journal of Biological Macromolecules, 146*, 821–831. https://doi.org/10.1016/j.ijbiomac.2019.10.050

Li, X., Manickavasagan, A., Lim, L.-T., & Ali, A. (2022). In A. Manickavasagan, L.-T. Lim, & A. Ali (Eds.), *171–196)Plant-based protein meat analogues - plant protein foods*. Springer International Publishing. https://doi.org/10.1007/978-3-030-91206-2_6.

Lin, D., Kelly, A. L., & Miao, S. (2021). Alginate-based emulsion micro-gel particles produced by an external/internal O/W/O emulsion-gelation method: Formation, suspension rheology, digestion, and application to gel-in-gel beads. *Food Hydrocolloids, 120*, Article 106926. https://doi.org/10.1016/j.foodhyd.2021.106926

Lin, D., Kelly, A. L., & Miao, S. (2022). The impact of pH on mechanical properties, storage stability and digestion of alginate-based and soy protein isolate-stabilized emulsion gel beads with encapsulated lycopene. *Food Chemistry, 372*, Article 131262.

Lu, Y., Mao, L., Hou, Z., Miao, S., & Gao, Y. (2019). Development of emulsion gels for the delivery of functional food ingredients: From structure to functionality. *Food Engineering Reviews, 11*(4), 245–258. https://doi.org/10.1007/s12393-019-09194-z

Manoi, K., & Rizvi, S. S. H. (2009). Emulsification mechanisms and characterizations of cold, gel-like emulsions produced from texturized whey protein concentrate. *Food Hydrocolloids, 23*(7), 1837–1847. https://doi.org/10.1016/j.foodhyd.2009.02.011

Manzoor, S., Masoodi, F. A., Naqash, F., & Rashid, R. (2022). Oleogels: Promising alternatives to solid fats for food applications. *Food Hydrocolloids for Health, 2*, Article 100058. https://doi.org/10.1016/j.fhfh.2022.100058

Martins, A. J., Vicente, A. A., Cunha, R. L., & Cerqueira, M. A. (2018). Edible oleogels: An opportunity for fat replacement in foods. *Food & Function, 9*(2), 758–773.

Mattice, K. D., & Marangoni, A. G. (2020). Physical properties of plant-based cheese products produced with zein. *Food Hydrocolloids, 105*, Article 105746. https://doi.org/10.1016/j.foodhyd.2020.105746

Nikoo, A. M., Kadkhodaee, R., Ghorani, B., Razzaq, H., & Tucker, N. (2018). Electrospray-assisted encapsulation of caffeine in alginate microhydrogels. *International Journal of Biological Macromolecules, 116*, 208–216. https://doi.org/10.1016/j.ijbiomac.2018.04.167

Ong, W.-D., Tey, B.-T., Quek, S. Y., Tang, S.-Y., & Chan, E.-S. (2015). Alginate-based emulsion template containing high oil loading stabilized by nonionic surfactants. *Journal of Food Science, 80*(1), E93–E100. https://doi.org/10.1111/1750-3841.12729

Park, C., & Maleky, F. (2020). A critical review of the last 10 years of oleogels in food. *Frontiers in Sustainable Food Systems, 139*.

Poyato, C., Ansorena, D., Berasategi, I., Navarro-Blasco, Í., & Astiasarán, I. (2014). Optimization of a gelled emulsion intended to supply ω-3 fatty acids into meat products by means of response surface methodology. *Meat Science, 98*(4), 615–621. https://doi.org/10.1016/j.meatsci.2014.06.016

Rezende, R. A., Bártolo, P. J., Mendes, A., & Filho, R. M. (2009). Rheological behavior of alginate solutions for biomanufacturing. *Journal of Applied Polymer Science, 113*(6), 3866–3871.

Ritchie, H., Rosado, P., & Roser, M. (2019). *Meat and dairy production. Our world in data*. https://ourworldindata.org/meat-production#citation.

Ruttarattanamongkol, K., Nor Afizah, M., & Rizvi, S. S. H. (2015). Stability and rheological properties of corn oil and butter oil emulsions stabilized with texturized whey proteins by supercritical fluid extrusion. *Journal of Food Engineering, 166*, 139–147. https://doi.org/10.1016/j.jfoodeng.2015.06.005

Sala, G., de Wijk, R. A., van de Velde, F., & van Aken, G. A. (2008). Matrix properties affect the sensory perception of emulsion-filled gels. *Food Hydrocolloids, 22*(3), 353–363. https://doi.org/10.1016/j.foodhyd.2006.12.009

Sala, G., van Vliet, T., Cohen Stuart, M. A., Aken, G. A. van, & van de Velde, F. (2009). Deformation and fracture of emulsion-filled gels: Effect of oil content and deformation speed. *Food Hydrocolloids, 23*(5), 1381–1393. https://doi.org/10.1016/j.foodhyd.2008.11.016

Sarmento, B., Ferreira, D., Veiga, F., & Ribeiro, A. (2006). Characterization of insulin-loaded alginate nanoparticles produced by ionotropic pre-gelation through DSC and FTIR studies. *Carbohydrate Polymers, 66*(1), 1–7. https://doi.org/10.1016/j.carbpol.2006.02.008

Sato, A. C. K., Moraes, K. E. F. P., & Cunha, R. L. (2014). Development of gelled emulsions with improved oxidative and pH stability. *Food Hydrocolloids, 34*, 184–192. https://doi.org/10.1016/j.foodhyd.2012.10.016

Shahbazi, M., Jäger, H., Chen, J., & Ettelaie, R. (2021). Construction of 3D printed reduced-fat meat analogue by emulsion gels. Part II: Printing performance, thermal, tribological, and dynamic sensory characterization of printed objects. *Food Hydrocolloids, 121*, Article 107054. https://doi.org/10.1016/j.foodhyd.2021.107054

Smet, K., Coudijzer, K., Fredrick, E., De Campeneere, S., De Block, J., Wouters, J., Raes, K., & Dewettinck, K. (2010). Crystallization behavior of milk fat obtained from linseed-fed cows. *Journal of Dairy Science, 93*(2), 495–505. https://doi.org/10.3168/jds.2009-2588

Song, H.-J., Grant, I., Rotondo, D., Mohede, I., Sattar, N., Heys, S. D., & Wahle, K. W. J. (2005). Effect of CLA supplementation on immune function in young healthy volunteers. *European Journal of Clinical Nutrition, 59*(4), 508–517. https://doi.org/10.1038/sj.ejcn.1602102

Tomaszewska-Gras, J. (2012). Detection of butter adulteration with water using differential scanning calorimetry. *Journal of Thermal Analysis and Calorimetry, 108*(2), 433–438. https://doi.org/10.1007/s10973-011-1913-y

Zhang, B., Guo, X., Zhu, K., Peng, W., & Zhou, H. (2015). Improvement of emulsifying properties of oat protein isolate–dextran conjugates by glycation. *Carbohydrate Polymers, 127*, 168–175. https://doi.org/10.1016/j.carbpol.2015.03.072

Zhao, X., Li, D., Wang, L., & Wang, Y. (2022). Rheological properties and microstructure of a novel starch-based emulsion gel produced by one-step emulsion gelation: Effect of oil content. *Carbohydrate Polymers, 281*, Article 119061. https://doi.org/10.1016/j.carbpol.2021.119061